Strong, Nonresonant Radiation Enhances *Cis*–*Trans* Photoisomerization of Stilbene in Solution

Jana L. van den Berg,[⊥] Kallie Ilene Neumann,[⊥] John A. Harrison, Hayley Weir, Edward G. Hohenstein, Todd J. Martinez, and Richard N. Zare*

ABSTRACT: Previously, it has been demonstrated that external electric fields may be used to exert control over chemical reactivity. In this study, the impact of a strong, nonresonant IR field (1064 nm) on the photoisomerization of *cis*-stilbene is investigated in cyclohexane solution. The design of a suitable reaction vessel for characterization of this effect is presented. The electric field supplied by the pulsed, near-IR radiation (ε_1 = 4.5 × 10^7 V/cm) enhances the *cis* → *trans* photoisomerization yield at the red edge of the absorption spectrum (wavelengths between 337 and 340 nm). Within the microliter focal volume, up to 75% of all *cis*-stilbene molecules undergo isomerization to *trans*-stilbene in the strong electric-field environment, indicating a significant increase relative to the 35% yield of *trans*-stilbene under field-free conditions. This result correlates with a 1–3% enhancement in the *trans*-stilbene concentration throughout the bulk solution. Theoretical analysis suggests that the observed change is the result of dynamic Stark shifting of the ground and first excited states, leading to a significant redshift in *cis*-stilbene's absorption spectrum. The predicted increase in the absorption cross section in this range of excitation wavelengths is qualitatively consistent with the experimental increase in *trans*-stilbene production.

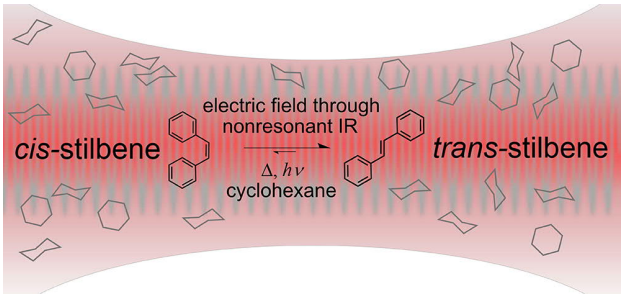

■ INTRODUCTION

Electrostatic interactions underlie all of chemistry. Beyond the complicated chemical equations and reaction schemes that are used to describe chemical reactions, it is the rearrangement of charges and their associated electric fields that govern chemical reactivity. This is the conceptual understanding from which we derive our electron-pushing mechanisms and rationalize how we get from starting material to product. Given that the probability and mechanism by which a reactant species is transformed into product is so dependent on the nature of the associated electric fields, it is unsurprising that modulating the electric-field environment about a reacting system can influence its outcome. Consider, for example, the well-modeled S_N2 reaction. This reaction, which involves the simultaneous breaking and forming of covalent bonds, is characterized by a highly polarizable, pentacoordinate transition state (TS). Because of enhanced delocalization of electrons relative to the reactant and product states, such transition states are susceptible to large changes in bond character (e.g., strength and ionicity). By lowering the relative energetic position of the TS, external electric fields have the potential to strongly influence reaction kinetics. In recent years, this insight has triggered experimental and computational inquiries into the possibility of electric-field assisted catalysis. A 2019 review article by Stuyver et al. provides a comprehensive overview of these studies.[1]

Perhaps the most compelling evidence for the impact of strong fields on chemical reactivity comes to us from nature: a collection of studies on enzymatic catalysis suggest that the catalytic function of many enzymes is significantly influenced by the localized electrostatic fields associated with charged functional groups within the protein. Using vibrational Stark spectroscopy, Boxer and co-workers have offered experimental support for this hypothesis by demonstrating a causal relationship between the strong electric fields (~10^7 V/cm) measured at active pockets and the catalytic rate.[2,3] The experimental findings of Spackman and co-workers further substantiate this result.[4] By performing high-resolution synchrotron and neutron charge density analysis on a host–guest system that models the substrate selectivity of enzymes, they observed measurable enhancement in the dipole moments associated with substrate molecules in the presence of a host.

The demonstration of electrostatic catalysis in condensed-phase environments extends beyond biological systems and into the chemical laboratory. Although the large field strengths

associated with enzymatic catalysis cannot be generated by typical static field sources, scanning tunneling microscope (STM) techniques allow for large, orienting electric fields ($\sim 10^7$–10^8 V/cm) to be generated in the small space between the STM tip and a substrate. Several studies using STM technology provide evidence for control over the rates of single-molecule reactions. In the first of these studies, Aragonés et al. demonstrated a 5-fold increase in the rate of bridge formation for the Diels–Alder reaction.[5] More recently, Zang et al. used a similar STM setup to show catalysis of the *cis*-to-*trans* isomerization of cumulenes in solution.[6] As is the case with enzymatic catalysis, the reactivity effects associated with application of these external electric fields via STM are attributed to the field-induced stabilization of polar or ionic transition states.[1]

An alternative approach to exploring the impacts of strong electric fields on chemical reactivity involves the use of light—specifically, coherent light from a laser beam. Light propagates through space as a wave of oscillating electric and magnetic fields. Exploration of the interactions between resonant light and matter has provided us with a wealth of structural and dynamical information. Largely overlooked, however, is the impact of *nonresonant* radiation, which, when introduced into a reaction system from an intense, pulsed laser beam, may induce changes in the system through its associated strong electric-field component.[7] To put the size of a laser's electric-field component into perspective, consider the following example: an IR laser pulse (1064 nm) of 500 mJ focused to a beam waist radius of 30 μm and having a duration of 10 ns has an electric field of $\varepsilon_0 = 5 \times 10^7$ V/cm. Because the beam is off-resonant to any of the transitions within the system, it changes the electrostatic characteristics of the environment without itself being used up: the nonresonant beam enters and exits the reaction volume, essentially unchanged. Drawing upon the parallels to a conventional chemical catalyst, an intense ($I = 10^{12}$ W/cm^2, $\varepsilon_0 = 10^7$ V/cm) nonresonant laser beam has been referred to as a "photonic catalyst."[8,9]

For nonresonant frequencies much greater than the reciprocal of the laser pulse duration, the first-order interaction between the permanent dipole moment of a molecule and the applied field averages to zero.[10] The AC field predominantly interacts instead with the dipole moment induced by the field—i.e., the polarizability of the evolving system—to dynamically Stark shift its potential energy surfaces. Under strong-field conditions ($\varepsilon_0 = 10^7$ V/cm), a sizable shift in the energy levels of the system may influence a reaction by enhancing certain reaction pathways relative to others and/or modifying the probabilities of resonant processes. For example, by shifting ground and excited surfaces relative to one another, it is possible to increase (or decrease) the absolute number of molecules that are excited in a photoinitiated process.[7] By effectively lowering an activation barrier to reaction, the electric field associated with pulsed, focused laser beams behaves analogously to the charged functional groups scattered throughout an enzyme and the voltages applied during electrocatalytic STM experiments. This analogy is particularly relevant when the field couples only with the molecular system's polarizability and thus follows the strong-field laser's envelope frequency. Unlike the carrier frequency, the envelope frequency is comparable to the low-frequency fluctuations of large biological molecules as well as the STM tip, as it is moved relative to a reactive substrate.

Stolow and co-workers were the first to demonstrate dynamic Stark control over reaction outcome via a non-resonant laser field. Upon application of a femtosecond, near-IR "control" pulse to the gas-phase photodissociation of IBr, they observed significant changes in the reaction's branching ratio relative to the field-free case.[9,11] Theoretical calculations provided support for the conclusion that this change was the result of a modification of the hopping probability between different excited states as IBr separated into its atomic constituents. In a handful of subsequent molecular beam experiments involving the photodissociation of diatomic[12] and polyatomic molecules,[13–15] various authors have reported changes to the reaction outcome consistent with laser-induced nonresonant modifications to absorbance spectra and conical intersection (CI) energies. These observations have been made using both nanosecond and ultrafast laser pulses to deliver the strong field and therefore reflect the impact of the electric field when it is applied over the course of the entire reaction as well as at specific time points. The general phenomenon of altering the reaction mechanism and/or outcome through application of a nonresonant laser pulse has been referred to as *laser-field catalysis*, or *photon catalysis*.[9,11]

In addition to Stark shifting energy levels, a strong AC field may cause a molecular system to become aligned. This orienting effect is like that observed in the STM experiments previously discussed.[5,6] The interaction between the AC field and the molecular polarizability leads to a mixing of J levels to create directional superpositions of the field-free eigenstates, or *pendular states*.[10,16–19] Specifically, matrix elements connect J to $J \pm 2$, i.e., even J levels with other even J levels and odd J levels with other odd J levels.[18] Because the $J = 0$ rotational level can only couple to $J = 2$, molecular alignment is most marked in rotationally cold environments where the majority of molecules occupy the ground rotational state. Although our previous molecular beam experiments did not provide the rotationally cold environment necessary for measurable alignment effects, others have demonstrated substantial alignment of linear molecules like iodine[20] and carbonyl sulfide[21] as well as more complex compounds like pyrimidine.[22] For reactions with competing anisotropic product channels, alignment, like dynamic Stark shifting, could theoretically be used to modify the outcome of collisional encounters.

Regardless of the specific mechanism(s) by which a nonresonant, AC field modifies a reaction, studies such as those referenced above offer a significant opportunity to build upon our fundamental understanding of the role of strong fields in modulating reaction kinetics. To our knowledge, all reported experimental investigations involving the electric field supplied by nonresonant radiation have been completed in the controlled environment of a molecular beam. By considering the impact of a nonresonant AC field on reactions in *liquid* media, the work outlined herein establishes a bridge between previous laser-field catalysis studies and studies that involve the effects of external DC fields on condensed-phase systems. This bridge, however, is not a simple one to construct. Solution-phase systems, for which we cannot control as precisely the "input state" and have less understanding about the impact of the medium, offer many additional challenges relative to molecular beam experiments. These challenges must be addressed in the design of the experiment. Because of greater density of molecules within the nonresonant laser's focal volume, heating effects can potentially lead to thermal changes

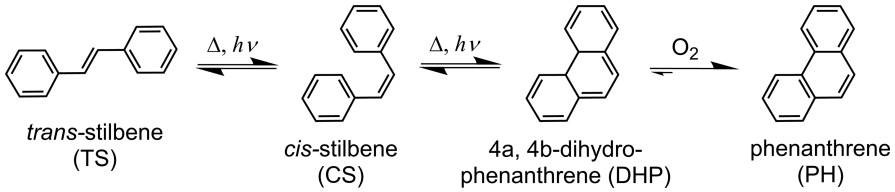

Figure 1. Light-induced isomerization of *cis*/*trans*-stilbene (CS/TS), and competing ring-closing reaction to produce DHP and PH.

in the solution's equilibrium state as well as to changes to the beam profile. These concerns must be met with careful consideration of the optical properties of the solvent. Furthermore, innovative engineering is required to develop a reaction vessel that balances the demand for high laser intensity with the damage thresholds of optical and carrier materials. These and other design considerations are elaborated upon in the Experimental Methods section of this report. Outside of the external, tangible challenges of the experiment, it must also be noted that, unlike the nearly collision-free conditions of molecular beam experiments, we can no longer neglect the contribution of the solvent's polarizability to the total field effect that we observe. Instead, we must regard the system as an extended chain or aggregate of molecules, rather than as a collection of isolated species.

Bearing these challenges in mind, the photoisomerization and ring-closing reactions of *cis*-stilbene have been chosen as the subject of our first investigation into the effect(s) of a nonresonant, AC field on a reaction in the solution phase. Stilbene exists in two isomeric forms, *cis* (CS) and *trans* (TS), which can be reversibly interconverted in the presence of ultraviolet (UV) light (Figure 1). CS can also undergo a ring-closing reaction to produce 4*a*,4*b*-dihydrophenanthrene (DHP). Under ambient conditions, DHP is entirely oxidized to the more stable aromatic species, phenanthrene (PH). Stilbene's isomerization is a classic example of a photochemical process that involves conical intersections. Therefore, it has been extensively studied, both theoretically and via a variety of experimental techniques, and its field-free dynamics provide a solid foundation for continuing studies.[23−35] Furthermore, because of the electron delocalization in stilbene's π system, the polarizability of the system is expected to change as it undergoes torsional motion and evolves along the reaction coordinate from reactants to products. This property of the reaction system increases the likelihood that the AC field will interact with the system to alter relative reaction yields.

Taking the *cis* isomer as the starting reagent, under field-free conditions, the reaction proceeds along two primary reaction pathways upon excitation to the first excited singlet state (Figure 2).[26] In the pathway leading toward TS, which accounts for the majority of the reaction, the molecule crosses a small activation barrier and twists into a low-energy perpendicular configuration that is rapidly converted to the ground state through a twisted/pyramidalized conical intersection.[29] The result of this pathway is that the excited molecule branches into its *cis* or *trans* forms with comparable yields. In an alternative reaction pathway, the excited *cis*-stilbene molecule moves toward a second conical intersection to undergo a ring-closing reaction to DHP.[30,33] The quantum yields of photoproducts under field-free conditions following excitation into the first singlet state of *cis*-stilbene have been measured to be 0.55 *cis*-stilbene, 0.35 *trans*-stilbene, and 0.10 DHP.[35]

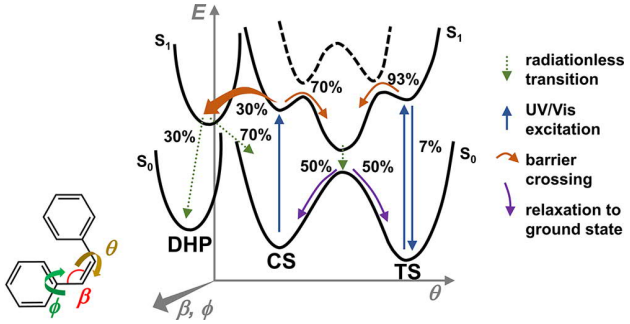

Figure 2. Schematic of stilbene's ground and first excited singlet states, S_0 and S_1, detailing the pathways and relative quantum yields for the isomerization and ring-closing reactions upon absorption of UV light.[26] θ is the rotation angle around the central double bond in the molecule, β is the bond angle between the benzene substituent and the central double bond, and φ is the rotational angle of the benzene substituent about the single bond.

The primary objective of this study is to investigate how the final product concentrations of *cis*-stilbene, *trans*-stilbene, and phenanthrene change with application of a nanosecond, nonresonant IR field to a dilute solution of *cis*-stilbene dissolved in cyclohexane. In what follows, we present the development of an experimental setup to investigate the effect of a nonresonant IR field on a reaction in solution and present results for the photoisomerization and ring-closing reactions of *cis*-stilbene both with and without an applied field. With the support of electronic structure calculations, we propose a mechanism by which the strong, nonresonant field leads to a measurable enhancement in *cis*−*trans* isomerization. Our theoretical treatment suggests that application of the field induces a dynamic Stark shift that results in an increase in absorption cross section at the experimental excitation wavelengths.

METHODS

I. Experimental Methods. A custom-engineered cell was filled with a dilute solution (8.5×10^{-6} M) of *cis*-stilbene (Sigma-Aldrich, 96%) in spectral-grade cyclohexane (Spectrum Chemicals). *Cis*-stilbene was selected over *trans*-stilbene as a starting material for these studies for two reasons. Stilbene is more weakly absorbing in the *cis* form; therefore, by starting with the *cis* isomer, it is possible to minimize absorption events occurring outside of the strong-field laser's focal volume. As the experiment proceeds, fresh solution diffusing into the focal volume may be approximated as an infinite source of *cis*-stilbene molecules rather than a mixture of the two isomers. Furthermore, by starting with *cis*-stilbene, we allowed for the possibility of observing the impact of the strong field on two competing reaction pathways—photoisomerization and photocyclization. Because we were seeking to investigate the impact of a *nonresonant* AC field on reaction outcome, cyclohexane

was chosen as a solvent. Cyclohexane does not exhibit any resonant transitions or overtone absorptions at the wavelength of the electric-field laser, 1064 nm, resulting in negligible absorbance at this wavelength. Importantly, cyclohexane is also transparent to the UV light used to promote the isomerization and ring-closing reactions.[32,36] In what follows, we describe the experimental setup from the vessel design to detection and quantification of stilbene products.

a. Vessel Design. Three primary considerations for vessel design were (i) the compatibility of construction materials with the chosen chemicals and laser wavelengths, (ii) the minimum distance required between the windows and the high-intensity focal region of the electric-field laser to prevent window damage, and (iii) the achievement of spatial overlap between the electric-field laser and the UV laser promoting excitation from S_0 to S_1. With these requisites in mind, the vessel's main body was constructed from two borosilicate glass tubes, each 5 cm long and 2 cm in diameter (Friedrich & Dimmock, Inc.). As indicated in Figure 3, the tubes were situated end-to-end

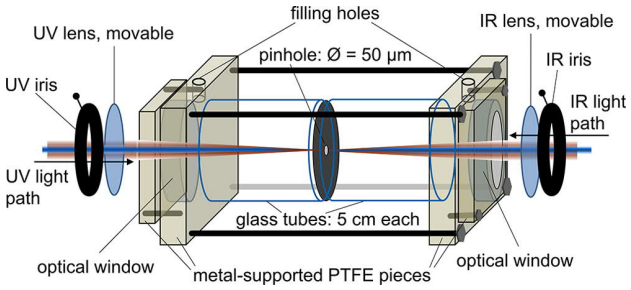

Figure 3. Schematic of the reaction vessel developed to investigate the impact of a nonresonant IR field on the photoisomerization and photocyclization reactions of *cis*-stilbene.

between two fitted polytetrafluorethylene (PTFE) pieces and sealed against calcium fluoride windows (Newport, Inc.) using Kalrez O-rings. The windows were tightened against the O-rings by metal-supported PTFE blocks. Solution was introduced into the reaction vessel via a syringe or a peristaltic pump through holes drilled into the tops of both PTFE pieces. The total volume of liquid contained by the vessel was approximately 25 mL. The large size of the cell relative to the focal volume of the electric-field laser contributes to a significant dilution of the possible effect, and the long path-length for the light to travel increases the probability of undesirable absorption processes; however, the cell dimensions outlined above were determined to be necessary to avoid damage to the optical windows.

Spatial overlap between the nonresonant electric-field laser and the UV photoexcitation laser was achieved by installing a high-damage threshold pinhole with a diameter of 50 μm (Thorlabs) between the two borosilicate tubes. It was secured to the glass with a two-component epoxy glue that exhibited high degradation resistance to cyclohexane and similar solvents (EP41S-5 and EP62-1HT, Master Bond Inc.).

b. Optical System: Electric-Field Laser and Ultraviolet Laser. The nonresonant infrared (IR) laser, which provided the strong electric field, and the ultraviolet (UV) laser, which promoted the excitation of *cis*-stilbene into its first excited electronic state, traveled in opposite directions through the vessel. They were overlapped spatially through a pinhole by adjusting the respective beam paths with movable lenses. Both lasers were focused at the pinhole's position to obtain the greatest field strength within the region of maximum overlap. Temporal overlap was achieved by relative delay of the trigger to one of the lasers and monitoring scattered light from the interaction region using a photodiode and oscilloscope.

The strong electric field was supplied by the near-IR fundamental of an Nd:YAG laser (Spectra Physics, GCR Series) at 1064 nm. This wavelength is not resonant with any of *cis*-stilbene's rovibrational transitions, which are reported to occur between approximately 3070 and 30 cm^{-1} for both the ground and first excited states.[37] The average pulse width produced by this laser is 10−12 ns; therefore, the field is "on" during the entire course of the 1 ps photoreaction.[35] For most experiments described herein, the peak power of the IR laser, measured prior to entering the cell, was 800 mW. This beam was focused with a 150 mm lens to a spot size in the micrometer regime. With the beam parameters provided, a spot size of 13.5 μm and a focal depth of 266 μm are predicted for vacuum conditions; however, in the liquid, the spot size was observed to increase with time through the process of thermal lensing. Therefore, the calculated field strength of $\varepsilon_l = 4.5 \times 10^7$ V/cm ($I = 1.1 \times 10^{13}$ W/cm^2) represents an upper limit on the field strength experienced by molecules within the focal region of the near-IR laser beam. Note that this value accounts for the refractive index of the solvent, cyclohexane, which lowers the electric-field strength by approximately a factor of 2. More details on the calculation of the electric-field strength's upper limit are provided in the SI.

Stilbene photoisomerization was promoted with UV radiation emitted from a tunable dye laser (Lambda Physik, LPD 3000), which was pumped by the second harmonic of an Nd:YAG laser (Spectra Physics, GCR Series), and subsequently frequency doubled, or tripled, by BBO crystals. The resulting UV pulse width was measured to be approximately 8 ns. For most experiments, the UV laser power was maintained between 12−15 μJ, or at 30 ($\pm$2) μJ, as noted in the Results and Discussion section. Most experiments were performed at the red edge of *cis*-stilbene's absorbance curve, between 337 and 340 nm, to minimize the number of isomerization and ring-closing events occurring outside of the focal volume of the electric-field laser (Figures S1 and S2). This decision was made because of practical limitations of the experimental setup: in the absence of the strong field, some amount of isomerization i is promoted by the UV light. When the IR is turned on, the amount of isomerization is $i + \Delta i$, where Δi is the change in the amount of isomerization that occurs in the microliter-sized volume in which the two lasers are focused and overlapped. Because of the approximately million-fold dilution of the focal volume relative to the entire cell volume, to make Δi detectable, i throughout the solution must be made as small as possible to achieve an observable effect. This condition is met when probing the edge of the molecule's absorbance spectrum rather than other parts of the spectrum.

c. Experimental Conditions. Five types of experiments were carried out, each for 1 h. Under field-free conditions, only the UV passed through the solution, and under strong-field conditions, the same experiment was repeated with simultaneous application of the nonresonant electric-field laser. In addition to field-free and nonresonant IR-field experiments, three control experiments were performed to gauge the extent to which the IR does not behave catalytically, i.e., is absorbed by species within the solution. Possible noncatalytic con-

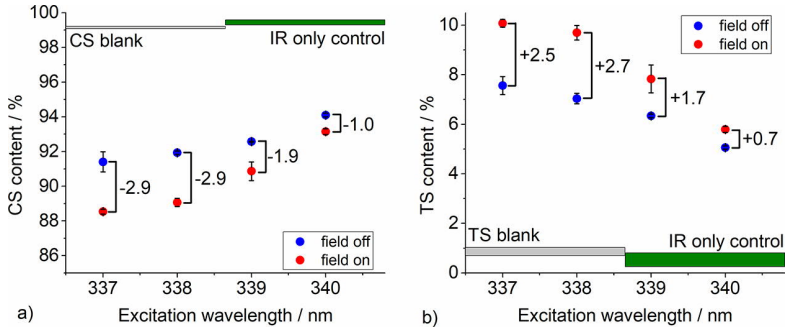

Figure 4. Effect of nonresonant IR field ($\varepsilon_0 \leq 4.5 \times 10^7$ V/cm) on the relative yields of (a) *cis*-stilbene and (b) *trans*-stilbene upon UV excitation between 337−340 nm. Experiments were performed on a solution of CS in spectral-grade cyclohexane. Blue and red dots represent data collected under field-free and strong-field conditions, respectively. The gray line describes the measured (a) CS or (b) TS content of the blank, a *cis*-stilbene solution not exposed to laser radiation. The green line describes the measured contents of each isomer with application of the IR laser only. Error bars represent 1 standard deviation from the mean of 3−7 data sets.

tributions of the IR include (1) participating in one-color or two-color multiphoton excitation processes and (2) heating the solution. Further explanation of each of the three control experiments as well as how they address the previously described noncatalytic contributions, is included within the Results and Discussion section. To determine the *cis*-stilbene content of the starting solution, as measured by absorbance, blank solutions that were not exposed to any irradiation except the ambient light from the room were worked up in the same way as experimental and control samples.

d. Sample Workup and Quantification of Reaction Products. After irradiation with UV and/or IR light for 1 h, each sample was removed from the reaction vessel, dried down under nitrogen gas, and reconstituted in acetonitrile. CS, TS, and PH were quantified using an HPLC (Waters) with photodiode array detector. Adequate separation of the three components was achieved using a silica-based pentafluorophenyl propyl (PFP) column and solvent gradient of methanol and acetonitrile. The photodiode array detector covered the range of absorption wavelengths from 210 to 500 nm so that the separated compounds could be identified by their absorption spectra. The following respective absorption maxima were used for quantification: 295 nm for TS, 280 nm for CS, and 251 nm for PH. Peak areas for CS, TS, and PH were integrated using instrument software. Concentrations of each species were determined by construction of calibration curves spanning the relevant concentration ranges, and relative yields are presented as normalized values. For example, for *cis*-stilbene, CS content is the concentration of CS over the sum of the concentrations of the three stilbene species. No other stilbene-related species were detected by this method.

II. Theoretical Methods. Because the dynamics of this reaction occur on a time scale that is orders of magnitude faster than the 10 ns IR laser pulse duration, we model the photoreaction with a new set of field-dressed curves that are effectively constant throughout the reaction. The energy of a system, E, in the presence of a time-independent electric field is given by

$$E = E_0 - \mu_0\varepsilon_0 - \frac{1}{4}\varepsilon_0 \cdot \alpha \cdot \varepsilon_0 \tag{1}$$

where E_0 is the energy of the system in zero field, μ_0 is the permanent dipole moment, ε_0 is the field vector, and α is the polarizability tensor.[38,39] The static polarizability, α, is defined as the second derivative of the energy of the system in the field or, equivalently, the first derivative of the dipole moment

$$\alpha = \frac{\mathrm{d}^2E}{\mathrm{d}{\varepsilon_0}^2} = \frac{\mathrm{d}\mu_0}{\mathrm{d}\varepsilon_0} \tag{2}$$

The Stark-shifted energy of each surface (eq 1) in the presence of the field is composed of the static Stark term, $-\mu_0\varepsilon_0$, and the dynamic Stark term, $-1/4\varepsilon_0\alpha\varepsilon_0$. Figure S3 shows that the second-order Stark effect is dominant for *cis*-stilbene at the field strength and carrier frequency used in the experiments described in this work. In magnitude, the first-order Stark shift to the S_0/S_1 energy gap is approximately 1/3 of the second-order Stark shift. More importantly, the first-order term oscillates, causing equal negative and positive shifts to the energy gap that, given our experimental parameters, would lead to an observation of no difference between the field-free and strong-field cases. Therefore, we assume that the static Stark term is completely averaged out by the high-frequency oscillations and consider only the dynamic Stark term in our calculations. The "field-off" energies, E_0, of the ground and excited surfaces are lowered by $1/4\varepsilon_0\alpha\varepsilon_0$. Modeling our system in this way, i.e., assuming negligible dipole coupling, is consistent with two previous demonstrations of the nonresonant dynamic Stark effect on polyatomic systems, the photodissociation of phenol and the photodissociation of methyl iodide.[13,14]

The polarizability tensor, α, of *cis*-stilbene was determined using a state-averaged complete active space self-consistent field (SA-2-CASSCF(2,2)) with an aug-cc-pVDZ spherical basis set.[29] We have previously shown that SA-2-CASSCF(2,2) provides a reliable description of the potential energy surface of *cis*-stilbene.[29] These calculations were performed on the B3LYP/6-31G* optimized ground-state *cis*-stilbene geometry. All quantum chemistry calculations were performed using the TeraChem quantum chemistry software.[40−42] We modeled the IR field ($\varepsilon_0 = 4.5 \times 10^7$ V/cm) perpendicular to the pump pulse by averaging over field vectors 20° apart in the plane perpendicular to the transition dipole moment. For each of the field vectors in the plane, we assumed a distribution of molecular orientations on a sphere using a Lebedev grid of order 35 with an orientation excitation probability according to $\cos^2\theta$ about the transition dipole moment. For each molecular orientation, the dynamically Stark-shifted S_0/S_1 energy gap was determined, and the *cis*-stilbene absorption spectrum was shifted by this value. The final dynamically Stark-shifted

absorption spectrum ("field on"), was obtained from an excitation probability-weighted average of the shifted absorption spectra (Figure S4).

RESULTS AND DISCUSSION

Dilute solutions of *cis*-stilbene in spectral-grade cyclohexane were irradiated with 12−15 μJ of UV light under both field-free and strong-field conditions. A focused near-IR laser (1064 nm) supplied the strong electric field. At excitation wavelengths on the red edge of *cis*-stilbene's absorption band, between 337−340 nm, the CS content was significantly reduced in the presence of a strong, nonresonant IR field (Figure 4a). A corresponding increase in the TS content (Figure 4b) is consistent with enhanced isomerization from *cis*-stilbene to *trans*-stilbene. The percent change in CS content ranges from 1% at 340 nm to 2.9% at 337 and 338 nm, revealing a general increase in the effect as excitation energy is increased. No effect on the isomerization is observed at UV wavelengths higher than 340 nm. Furthermore, unlike the two stilbene isomers, the concentration of phenanthrene is not measurably altered under any of these experimental conditions (Figure S5).

At less than a 5% change, the measured increase in isomerization may at first seem insignificant; however, when the practical limitations of the experimental setup are considered, it represents a substantial increase in photoisomerization. As noted in the Experimental Methods section, the large volume of the reaction vessel relative to the focal volume of the electric-field laser significantly dilutes the possible effect: with each laser shot, only one-millionth of the total vessel volume experiences the strongest possible electric field at the focal point of the near-IR laser. Previous experiments in the gas phase suggest that, outside of the focal region, the electric field would not be strong enough to induce measurable change to the reaction dynamics.[12,13] Assuming that the solution within the focal volume is replaced between each laser shot, consistent with a mass diffusion constant of approximately 10^{-5} cm^2/s,[43] and that 100% of the *cis*-stilbene molecules within that volume undergo isomerization, the maximum possible enhancement that we could observe for a 1 h experiment (repetition rate = 10 Hz) is approximately 4%. Given the 3% change that is observed at 337 and 338 nm excitation, these results suggest that, within the microliter focal volume, up to 75% of all *cis*-stilbene molecules are undergoing isomerization to *trans*-stilbene in the strong electric-field environment.

The dramatic increase in isomerization yield within the focal volume prompts questions regarding the extent to which the near-IR laser is truly behaving nonresonantly, i.e., is providing a strong electric-field environment without being absorbed to a significant extent. As the green line in Figure 4 indicates, IR-only control experiments reveal that no detectable conversion from the starting material occurs as the result of multiphoton absorption of IR photons or thermal isomerization by absorption of the IR alone. Other possible nonresonant or *noncatalytic* contributions of the 1064 nm IR laser include (a) two-color, two-photon absorption (TPA) and (b) heat-induced changes in the absorption cross section of the stilbene isomers. To address these possibilities, two sets of control experiments were performed at one representative wavelength, 338 nm. For these control experiments, detailed below, the UV laser power was maintained at 30 μJ (compared to 12−15 μJ used for experimental conditions). Schematic representations of these control conditions are provided in Figure S6.

An experiment in which the relative polarization of the two lasers was changed probed the TPA contribution of UV + IR multiphoton processes. This control experiment assumes that rotation of a *cis*-stilbene molecule occurs more slowly than it can absorb both a UV and IR photon to promote an isomerization event. Based upon measurements for *trans*-stilbene in hexane solvent, the rotational reorientation time of *cis*-stilbene is estimated to be more than 1 order of magnitude greater than its isomerization lifetime (15 vs 1 ps); consequently, this is a valid assumption for this system.[35,44] There are not significant differences in depletion of CS content under parallel vs perpendicular polarization conditions (Figure 5, right vs center), indicating that two-color, two-photon multiphoton absorption is not responsible for the observed enhancement in CS isomerization.

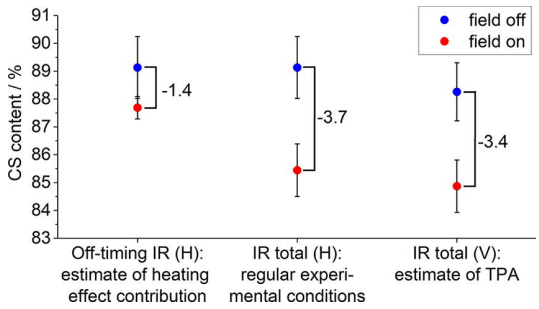

Figure 5. CS yields for 338 nm photoisomerization of stilbene under strong-field (red) and field-free (blue) conditions. Left side: Estimate of local heating effects by comparing the effect of a time-delayed IR (left) with the regular experimental conditions (center). Right side: Estimate of two-photon absorption (TPA) through comparison of experiments with a horizontally polarized UV beam (H) and a vertically polarized UV beam (V). The error bars correspond to one standard deviation over three experimental data sets.

In a second control experiment, in what is referred to as the "off-timing" condition, the IR laser was offset in time by 100 ns before or after the UV pulse. Neither multiphoton absorption nor any catalytic impacts of the strong field can be observed when the lasers are not temporally overlapped; however, given that the thermal diffusivity constant of cyclohexane is on the order of 10^{-5} μm^2/ns, a 100 ns delay adequately captures background associated with thermal changes to overall reaction yields.[45] Figure 5 reveals that when the pulses are not overlapped in time, a small amount of CS depletion is still observed relative to the field-free condition (Figure 5, left vs center). The magnitude of the corresponding enhancement in CS to TS isomerization is independent of whether the 10 ns IR pulse is placed before or after the UV pulse in time. For the representative excitation wavelength of 338 nm, 38% of the total effect is attributed to heating.

The measurable increase in TS production in the "off-timing" experiment suggests that, in the presence of the strong IR field, the reaction solution experiences (a) shifts in the thermal reaction equilibrium and/or (b) heat-induced changes to the molecule's absorption cross section. We visually observed thermal lensing throughout the solution, which supports the establishment of a thermal equilibrium along the beam path at an elevated temperature relative to the bulk solution. Analysis of the temperature dependence of *cis*-

stilbene's absorption spectrum reveals minor changes to the absorptivity within the experimental wavelength range (Figure S1). Therefore, control data suggests that a shift in the equilibrium is primarily responsible for the observed heating effects. Despite the nonzero thermal contribution to the observed enhancement in the amount of isomerization, conversion is still significantly greater when the two laser pulses are overlapped in time. Given that most of the observed effect is neither connected to absorption of IR photons nor heating of the reaction solution, the primary mechanism of change must stem from the strong-field environment supplied by the nonresonant IR laser.

In addition to the nonresonant dynamic Stark effect mentioned in the Introduction, there are a few other possible impacts of a strong field that must be evaluated for a thorough interpretation of the experimental results. This becomes increasingly true when we consider the complex nature of the problem: a reaction occurring in condensed media. To begin, let us consider rapid adiabatic passage, a technique that provides an efficient way to induce complete population transfer between two bound states of a quantum system.[46] Typically, this population change is accomplished by simultaneously (a) sweeping the carrier frequency of a laser pulse through resonance via a strong AC field and (b) varying the strength of the interaction. When the adiabatic following condition is met, i.e., when the interaction changes sufficiently slowly, so that the time evolution is adiabatic, there will occur a complete population transfer between states. For the stilbene system, meeting this condition for adiabatic passage would require that the field be "turned on" as the wavepacket evolves in time near the vicinity of the *cis/trans* CI. In our experiments, the strong field is "on" during the entire course of the reaction: we have effectively a new set of field-dressed curves that are constant over the time scale of the photoreaction's dynamics. Therefore, we are not able to sweep these surfaces into resonance in a time-dependent way to promote adiabatic transfer of population. At most, the energy gap between surfaces could be shifted into resonance with the NIR photon, resulting in stimulated emission pumping back down into the ground state prior to the wavepacket reaching the *cis/trans* CI. In this case, TS production would be inhibited rather than enhanced in the presence of the strong field; therefore, the observed trend is not explained via this mechanism.

Passage of an intense near-IR beam through a weakly absorbing medium also imposes local changes in the medium's index of refraction that contribute to modification of the UV laser's polarization (optical Kerr effect rotation) and phase (cross-phase modulation) relative to the field-free condition. The optical Kerr effect (OKE) describes the introduction of anisotropy into the medium by the AC field associated with pulsed radiation.[47] Experimentally, the induced birefringence is detected by observing the rotation of the coinciding UV beam through crossed polarizers.[48] In our setup, we attempted to quantify optical Kerr rotation in this way, as a means of improving the overlap condition between our two lasers, but were unsuccessful. This result suggests that, in our liquid-phase system, molecular alignment does not occur to a significant extent: the potential well depth created by the 1064 nm laser field is small compared to the thermal energy of the molecules at and above room temperature. Even if substantial alignment were anticipated, the well-established negative correlation between stilbene's *cis*−*trans* isomerization rate and viscosity of the solvent indicates that TS production would likely be suppressed rather than enhanced in the presence of an orienting electric field.[49] Note that we do not consider the possibility that a rotation of the UV beam's polarization itself leads to an enhancement in absorption of the UV photons. As Figure 5 shows, field-free experiments conducted with both vertical and horizontal polarizations of the UV light do not give significantly different isomerization yields.

Alternatively, cross-phase modulation (XPM) or, more aptly, imposed-phase modulation (IPM) refers to a change of one beam's phase because of a second beam passing through the Kerr medium.[50,51] Possible effects of XPM/IPM include spectral broadening of the UV excitation pulse as well as a frequency shift in the UV pulse's wavelength. Unfortunately, it is not possible to experimentally disentangle the effects of XPM from the impact of a dynamic Stark shift on the ground and excited surfaces. However, as theoretical calculations will show, our experimental results can be fully explained via a dynamic Stark shift of the S_1 and S_0 surfaces relative to one another; therefore, we exclude XPMs as the primary cause of the observed enhancement in isomerization.

There are at least three possible ways that a nonresonant dynamic Stark shift could lead to the observed enhancement in *cis*-to-*trans* isomerization

(1) The two surfaces are shifted in energy relative to one another at the Franck−Condon (FC) point, leading to an increase in the absolute number of molecules excited from the ground state.

(2) The geometry at the twisted/pyramidalized CI is altered, e.g., with an introduction of asymmetry, causing the pathway toward the *trans*-isomer to become more favorable than that toward the *cis*-isomer.

(3) There is a change in ratio between the barrier heights to the *trans*/*cis* CI and the DHP/*cis* CI, meaning that population that would normally proceed via one pathway takes the alternative pathway.

Because we probed this photoreaction between 337 and 340 nm, at the extreme red edge of the absorption spectrum, we primarily attribute the enhanced isomerization to the first of these mechanisms, i.e., a large increase in the absorption cross section. Electronic structure calculations (as described in the Theoretical Methods section) were used to calculate the absorption spectrum of *cis*-stilbene with application of an IR field (Figure 6). In the presence of the field, the absorption spectrum is shifted to lower energies, resulting in a significantly larger absorption cross section over the range of excitation energies used in this study. As a result, more *cis*-stilbene molecules are excited in the presence of the field, in comparison to when the field is turned off; therefore, the absolute number of molecules undergoing isomerization increases. From a qualitative standpoint, this supports the dramatic enhancement in TS production that is occurring within the focal volume of the IR laser and suggests that the other two possible mechanisms described above are insignificant in comparison to the overall effect. Furthermore, it is consistent with an experimentally observed trend: the enhancement in TS production decreases with an increase in excitation wavelength from 337−340 nm. Time-resolved, ultrafast spectroscopic techniques would be necessary to fully characterize the field-catalyzed reaction: by supplying the near-IR pulse at different delay times relative to the UV pulse, one could access different portions of the potential surface as the reaction occurs.

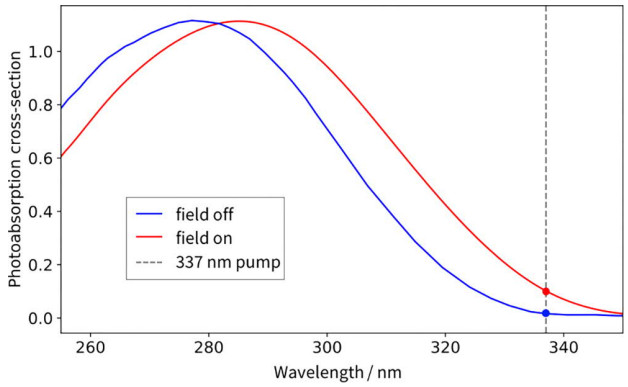

Figure 6. Absorption spectrum of *cis*-stilbene (blue, "field off") and the theoretical dynamically Stark-shifted spectrum when a nonresonant AC field is applied (red, "field on"). A pump wavelength of 337 nm (gray, dashed) is shown for reference to illustrate the expected increase in photoabsorption cross section with application of a field. Both spectra are normalized according to their area.

As alluded to previously, the decision to probe the red edge of the absorption curve was made to minimize the number of isomerization and cyclization events occurring outside of the focal region of the near-IR laser. In this way, we sought to enhance our sensitivity by targeting an on/off threshold effect. However, performing these experiments at additional wavelengths within the molecule's absorption curve would provide more data points to compare against the theoretical Stark shifting of the absorbance spectrum. Furthermore, operating well within the absorbance range for *cis*-stilbene offers the possibility to observe how the field could influence the reaction in other ways, i.e., by changing the relative activation barrier heights and/or the CI geometries. Therefore, experiments were repeated at 280 nm, near the peak of *cis*-stilbene's field-free absorbance band, and at 258 nm, on the rising edge of the curve. Unfortunately, at each of the wavelengths, non-negligible contributions from both two-photon absorption processes and thermal isomerization events were observed (Figures S7 and Figure S8). The enhanced thermal contribution relative to the edge wavelengths is consistent with experimentally collected temperature-dependent absorbance spectra (Figure S1). Thus, no statement can be made regarding the strong-field effect at these wavelengths. However, results of polarization dependence measurements at 258 nm (Figure S8) provide confidence in the reliability of the designed control experiment, as they confirm its ability to capture differences in isomerization yield between field-free and strong-field conditions when non-negligible multiphoton absorption events (1UV + 1NIR) are occurring.

CONCLUSIONS

Previously, it has been demonstrated that external electric fields may be used to exert control over chemical reactivity. In this work, a novel experimental setup was employed to investigate the impact of the strong electric field from nonresonant, pulsed radiation on the extent of photoisomerization of *cis*-stilbene in solution. Despite the challenges and constraints presented by the liquid environment, we demonstrated between 337−340 nm that the photoisomerization from *cis*-stilbene to *trans*-stilbene was significantly enhanced within the focal volume of the electric-field laser. These results are qualitatively consistent with electronic structure calculations, which predict an increased photoabsorption cross section at the experimental excitation wavelengths. Control experiments confirmed that one- and two-color multiphoton processes contributed negligibly to the observed effect. The thermal contributions to *trans*-stilbene production were measured, and they were small enough to be subtracted under these experimental conditions. Future work may focus on the impact of solvent properties (polarizability, orientation) in enhancing or mitigating the observed effect. The authors further encourage the use of time-resolved, ultrafast laser spectroscopy to probe the impact of the nonresonant IR field on different portions of the potential energy surface (e.g., reaction initiation, conical intersection, excited-state barriers) as the reaction proceeds in the solution phase.

AUTHOR INFORMATION

Corresponding Author

Richard N. Zare − *Department of Chemistry, Stanford University, Stanford, California 94305, United States;* orcid.org/0000-0001-5266-4253; Email: rnz@stanford.edu

Authors

Jana L. van den Berg − *Department of Chemistry, Stanford University, Stanford, California 94305, United States*

Kallie Ilene Neumann − *Department of Chemistry, Stanford University, Stanford, California 94305, United States*

John A. Harrison − *Department of Chemistry, Stanford University, Stanford, California 94305, United States; Chemistry, School of Natural and Computational Sciences, Massey University Auckland, Auckland 4442, New Zealand*

Hayley Weir − *Department of Chemistry, Stanford University, Stanford, California 94305, United States; SLAC National Accelerator Laboratory, Menlo Park, California 94025, United States;* orcid.org/0000-0002-1039-327X

Edward G. Hohenstein − *SLAC National Accelerator Laboratory, Menlo Park, California 94025, United States;* orcid.org/0000-0002-2119-2959

Todd J. Martinez − *Department of Chemistry, Stanford University, Stanford, California 94305, United States; SLAC National Accelerator Laboratory, Menlo Park, California 94025, United States;* orcid.org/0000-0002-4798-8947

Author Contributions

[⊥]J.L.B. and K.I.N. contributed equally to this research.

Notes

The authors declare no competing financial interest.

■ ACKNOWLEDGMENTS

R.N.Z., K.I.N., and J.L.B. were supported by the National Science Foundation under Grant No. 1464640. K.I.N. was also supported by the Center for Molecular Analysis and Design. T.J.M., E.G.H., and H.W. were supported by the AMOS program of the U.S. Department of Energy, Office of Science, Basic Energy Sciences, Chemical Sciences, and Biosciences Division.

■ REFERENCES

(1) Stuyver, T.; Danovich, D.; Joy, J.; Shaik, S. External Electric Field Effects on Chemical Structure and Reactivity. *Wiley Interdiscip. Rev.: Comput. Mol. Sci.* **2020**, *10*, e1438.

(2) Fried, S. D.; Bagchi, S.; Boxer, S. G. Extreme Electric Fields Power Catalysis in the Active Site of Ketosteroid Isomerase. *Science* **2014**, *346*, 1510−1513.

(3) Fried, S. D.; Boxer, S. G. Electric Fields and Enzyme Catalysis. *Annu. Rev. Biochem.* **2017**, *86*, 387−415.

(4) Shi, M. W.; Thomas, S. P.; Hathwar, V. R.; Edwards, A. J.; Piltz, R. O.; Jayatilaka, D.; Koutsantonis, G. A.; Overgaard, J.; Nishibori, E.; Iversen, B. B.; et al. Measurement of Electric Fields Experienced by Urea Guest Molecules in the 18-Crown-6/Urea (1:5) Host-Guest Complex: An Experimental Reference Point for Electric-Field-Assisted Catalysis. *J. Am. Chem. Soc.* **2019**, *141*, 3965−3976.

(5) Aragonès, A. C.; Haworth, N. L.; Darwish, N.; Ciampi, S.; Bloomfield, N. J.; Wallace, G. G.; Diez-Perez, I.; Coote, M. L. Electrostatic Catalysis of a Diels−Alder Reaction. *Nature* **2016**, *531*, 88−91.

(6) Zang, Y.; Zou, Q.; Fu, T.; Ng, F.; Fowler, B.; Yang, J.; Li, H.; Steigerwald, M. L.; Nuckolls, C.; Venkataraman, L. Directing Isomerization Reactions of Cumulenes with Electric Fields. *Nat. Commun.* **2019**, *10*, 4482.

(7) Bradshaw, D. S.; Forbes, K. A.; Andrews, D. L. Off-Resonance Control and All-Optical Switching: Expanded Dimensions in Nonlinear Optics. *Appl. Sci.* **2019**, *9*, 4252.

(8) Townsend, D.; Sussman, B. J.; Stolow, A. A Stark Future for Quantum Control. *J. Phys. Chem. A* **2011**, *115*, 357−373.

(9) Sussman, B. J.; Townsend, D.; Ivanov, M. Y.; Stolow, A. Dynamic Stark Control of Photochemical Processes. *Science* **2006**, *314*, 278−281.

(10) Friedrich, B.; Herschbach, D. Polarization of Molecules Induced by Intense Nonresonant Laser Fields. *J. Phys. Chem.* **1995**, *99*, 15686−15693.

(11) Stolow, A. Quantum Control: May the Electric Force Be With You. *Nat. Chem.* **2014**, *6*, 759−760.

(12) Hilsabeck, K. I.; Meiser, J. L.; Sneha, M.; Balakrishnan, N.; Zare, R. N. Photon Catalysis of Deuterium Iodide Photodissociation. *Phys. Chem. Chem. Phys.* **2019**, *21*, 14195−14204.

(13) Hilsabeck, K. I.; Meiser, J. L.; Sneha, M.; Harrison, J. A.; Zare, R. N. Nonresonant Photons Catalyze Photodissociation of Phenol. *J. Am. Chem. Soc.* **2019**, *141*, 1067−1073.

(14) Corrales, M.; González-Vázquez, J.; Balerdi, G.; Solá, I.; De Nalda, R.; Bañares, L. Control of Ultrafast Molecular Photodissociation by Laser-Field-Induced Potentials. *Nat. Chem.* **2014**, *6*, 785−790.

(15) Corrales, M. E.; de Nalda, R.; Bañares, L. Strong Laser Field Control of Fragment Spatial Distributions from a Photodissociation Reaction. *Nat. Commun.* **2017**, *8*, 1345.

(16) Friedrich, B.; Herschbach, D. R. Spatial Orientation of Molecules in Strong Electric Fields and Evidence for Pendular States. *Nature* **1991**, *353*, 412−414.

(17) Rost, J.; Griffin, J.; Friedrich, B.; Herschbach, D. Pendular States and Spectra of Oriented Linear Molecules. *Phys. Rev. Lett.* **1992**, *68*, 1299−1302.

(18) Friedrich, B.; Herschbach, D. Alignment and Trapping of Molecules in Intense Laser Fields. *Phys. Rev. Lett.* **1995**, *74*, 4623−4626.

(19) Ortigoso, J.; Rodríguez, M.; Gupta, M.; Friedrich, B. Time Evolution of Pendular States Created by the Interaction of Molecular Polarizability with a Pulsed Nonresonant Laser Field. *J. Chem. Phys.* **1999**, *110*, 3870−3875.

(20) Larsen, J. J.; Sakai, H.; Safvan, C.; Wendt-Larsen, I.; Stapelfeldt, H. Aligning Molecules with Intense Nonresonant Laser Fields. *J. Chem. Phys.* **1999**, *111*, 7774−7781.

(21) Sakai, H.; Minemoto, S.; Nanjo, H.; Tanji, H.; Suzuki, T. Controlling the Orientation of Polar Molecules with Combined Electrostatic and Pulsed, Nonresonant Laser Fields. *Phys. Rev. Lett.* **2003**, *90*, 083001.

(22) Franks, K. J.; Li, H.; Kong, W. Orientation of Pyrimidine in the Gas Phase Using a Strong Electric Field: Spectroscopy and Relaxation Dynamics. *J. Chem. Phys.* **1999**, *110*, 11779−11788.

(23) Momicchioli, F.; Bruni, M. C.; Baraldi, I.; Corradini, G. R. Mechanism of the Direct Trans→Cis Photoisomerization of Stilbene. Part 1.—Potential Energy Surfaces of the Lowest Excited States. *J. Chem. Soc., Faraday Trans. 2* **1974**, *70*, 1325−1333.

(24) Momicchioli, F.; Corradini, G. R.; Bruni, M. C.; Baraldi, I. Mechanism of the Direct Trans→Cis Photoisomerization of Stilbene. Part 2.—Thermally Activated Intersystem Crossing. *J. Chem. Soc., Faraday Trans. 2* **1975**, *71*, 215−224.

(25) Sension, R. J.; Repinec, S. T.; Hochstrasser, R. M. Femtosecond Laser Study of Energy Disposal in the Solution Phase Isomerization of Stilbene. *J. Chem. Phys.* **1990**, *93*, 9185−9188.

(26) Frederick, J. H.; Fujiwara, Y.; Penn, J. H.; Yoshihara, K.; Petek, H. Models for Stilbene Photoisomerization: Experimental and Theoretical Studies of the Excited-State Dynamics of 1,2-Diphenylcycloalkenes. *J. Phys. Chem.* **1991**, *95*, 2845−2858.

(27) Sension, R. J.; Repinec, S. T.; Szarka, A. Z.; Hochstrasser, R. M. Femtosecond Laser Studies of the Cis-Stilbene Photoisomerization Reactions. *J. Chem. Phys.* **1993**, *98*, 6291−6315.

(28) Baskin, J. S.; Bañares, L.; Pedersen, S.; Zewail, A. H. Femtosecond Real-Time Probing of Reactions. 20. Dynamics of Twisting, Alignment, and IVR in the Trans-Stilbene Isomerization Reaction. *J. Phys. Chem.* **1996**, *100*, 11920−11933.

(29) Quenneville, J.; Martínez, T. J. Ab Initio Study of Cis−Trans Photoisomerization in Stilbene and Ethylene. *J. Phys. Chem. A* **2003**, *107*, 829−837.

(30) Fuß, W.; Kosmidis, C.; Schmid, W. E.; Trushin, S. A. The Photochemical Cis−Trans Isomerization of Free Stilbene Molecules Follows a Hula-Twist Pathway. *Angew. Chem., Int. Ed.* **2004**, *43*, 4178−4182.

(31) Bao, J.; Minitti, M. P.; Weber, P. M. Ring-Closing and Dehydrogenation Reactions of Highly Excited Cis-Stilbene: Ultrafast Spectroscopy and Structural Dynamics. *J. Phys. Chem. A* **2011**, *115*, 1508−1515.

(32) Dobryakov, A. L.; Ioffe, I.; Granovsky, A. A.; Ernsting, N. P.; Kovalenko, S. A. Femtosecond Raman Spectra of Cis-Stilbene and Trans-Stilbene with Isotopomers in Solution. *J. Chem. Phys.* **2012**, *137*, 244505.

(33) Nakamura, T.; Takeuchi, S.; Taketsugu, T.; Tahara, T. Femtosecond Fluorescence Study of the Reaction Pathways and Nature of the Reactive S1 State of Cis-Stilbene. *Phys. Chem. Chem. Phys.* **2012**, *14*, 6225−6232.

(34) Ioffe, I. N.; Granovsky, A. A. Photoisomerization of Stilbene: The Detailed XMCQDPT2 Treatment. *J. Chem. Theory Comput.* **2013**, *9*, 4973−4990.

(35) Todd, D. C.; Jean, J. M.; Rosenthal, S. J.; Ruggiero, A. J.; Yang, D.; Fleming, G. R. Fluorescence Upconversion Study of Cis-Stilbene Isomerization. *J. Chem. Phys.* **1990**, *93*, 8658−8668.

(36) Pickett, L. W.; Muntz, M.; McPherson, E. M. Vacuum Ultraviolet Absorption Spectra of Cyclic Compounds. I. Cyclohexane,

Cyclohexene, Cyclopentane, Cyclopentene and Benzene. *J. Am. Chem. Soc.* **1951**, *73*, 4862−4865.
(37) Choi, C. H.; Kertesz, M. Conformational Information from Vibrational Spectra of Styrene, Trans-Stilbene, and Cis-Stilbene. *J. Phys. Chem. A* **1997**, *101*, 3823−3831.
(38) Liptay, W. Electrochromism and Solvatochromism. *Angew. Chem., Int. Ed. Engl.* **1969**, *8*, 177−188.
(39) Sussman, B. J. Five Ways to the Nonresonant Dynamic Stark Effect. *Am. J. Phys.* **2011**, *79*, 477−484.
(40) Ufimtsev, I. S.; Martínez, T. J. Quantum Chemistry on Graphical Processing Units. 1. Strategies for Two-Electron Integral Evaluation. *J. Chem. Theory Comput.* **2008**, *4*, 222−231.
(41) Ufimtsev, I. S.; Martinez, T. J. Quantum Chemistry on Graphical Processing Units. 2. Direct Self-Consistent-Field Implementation. *J. Chem. Theory Comput.* **2009**, *5*, 1004−1015.
(42) Ufimtsev, I. S.; Martinez, T. J. Quantum Chemistry on Graphical Processing Units. 3. Analytical Energy Gradients, Geometry Optimization, and First Principles Molecular Dynamics. *J. Chem. Theory Comput.* **2009**, *5*, 2619−2628.
(43) Kowert, B. A.; Dang, N. C.; Sobush, K. T.; Seele, L. G. Diffusion of Aromatic Hydrocarbons in n-Alkanes and Cyclohexanes. *J. Phys. Chem. A* **2001**, *105*, 1232−1237.
(44) Courtney, S. H.; Kim, S. K.; Canonica, S.; Fleming, G. R. Rotational Diffusion of Stilbene in Alkane and Alcohol Solutions. *J. Chem. Soc., Faraday Trans. 2* **1986**, *82*, 2065−2072.
(45) Watanabe, H.; Kato, H. Thermal Conductivity and Thermal Diffusivity of Twenty-Nine Liquids: Alkenes, Cyclic (Alkanes, Alkenes, Alkadienes, Aromatics), and Deuterated Hydrocarbons. *J. Chem. Eng. Data* **2004**, *49*, 809−825.
(46) Vitanov, N. V.; Halfmann, T.; Shore, B. W.; Bergmann, K. Laser-Induced Population Transfer by Adiabatic Passage Techniques. *Annu. Rev. Phys. Chem.* **2001**, *52*, 763−809.
(47) Li, C. *Nonlinear Optics: Principles and Applications*; Springer Singapore: Singapore, 2017.
(48) Righini, R. Ultrafast Optical Kerr Effect in Liquids and Solids. *Science* **1993**, *262*, 1386−1390.
(49) Nikowa, L.; Schwarzer, D.; Troe, J.; Schroeder, J. Viscosity and Solvent Dependence of Low-Barrier Processes: Photoisomerization of Cis-Stilbene in Compressed Liquid Solvents. *J. Chem. Phys.* **1992**, *97*, 4827−4835.
(50) Baldeck, P.; Ho, P. P.; Alfano, R. R. Effects of Self, Induced and Cross Phase Modulations on the Generation of Picosecond and Femtosecond White Light Supercontinua. *Rev. Phys. Appl.* **1987**, *22*, 1677−1694.
(51) Alfano, R. R.; Agrawal, G. P.; Baldeck, P. L.; Ho, P. P. Cross-Phase Modulation and Induced Focusing Due to Nonlinearities in Optical Fibers and Bulk Materials. *J. Opt. Soc. Am. B* **1989**, *6*, 824−829.